A Reactive Force Field with Coarse-Grained Electrons for Liquid Water

Itai Leven[1,2,5] , Hongxia Hao[1,2,5], Akshaya Kumar Das[1,2] and Teresa Head-Gordon[1,2,3,4,5*]

[1]Kenneth S. Pitzer Center for Theoretical Chemistry, [2]Department of Chemistry, [3]Department of Bioengineering, [4]Department of Chemical and Biomolecular Engineering
University of California Berkeley
[5]Chemical Sciences Division, Lawrence Berkeley National Laboratory
Berkeley, California 94720, USA

ABSTRACT

Non-reactive force fields are defined by perturbations of electron density that are relatively small, whereas chemical reactivity involves wholesale electronic rearrangements that make and break bonds. Thus reactive force fields are incredibly difficult to develop compared to non-reactive force fields, and yet at the same time they fill a critical need when *ab initio* molecular dynamics methods are not affordable. We introduce a new reactive force field model for water that combines modified non-bonded terms of the ReaxFF model and its embedding in the electrostatic interactions described by our recently introduced coarse-grained electron model (C-GeM). The ReaxFF/C-GeM force field is characterized for many energetic and dissociative water properties for water clusters, structure and dynamical properties at ambient conditions in the condensed phase, as well the temperature dependence of density and water diffusion, with very good agreement with experiment. The ReaxFF/C-GeM should be more transferable and more broadly applicable to a range of reactive systems involving both proton and electron transfer in the condensed phase.

*corresponding author: thg@berkeley.edu

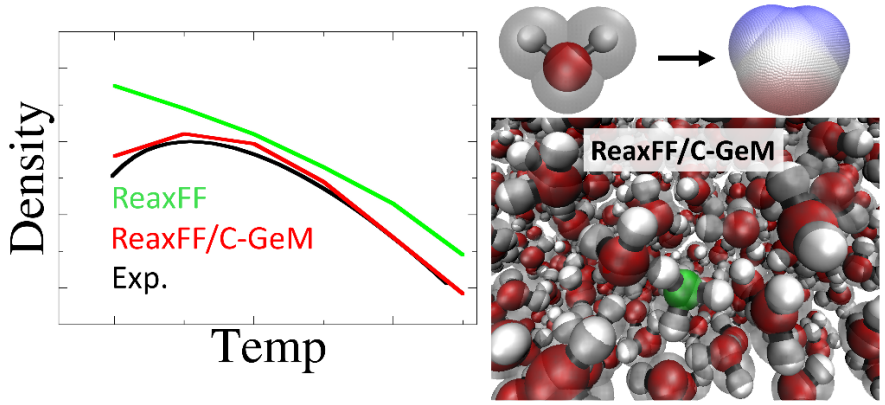

Key words: ReaxFF, C-GeM, Charge equilibration, Water force field, Explicit electrons

The water molecule is deceptively simple, but its interactions in the condensed phase have been found to be complex, exhibiting water anomalies such as temperature of maximum density, an unusually high melting point and surface tension, and the numerous structures of ice, triggering extensive scientific research for more than a century.[1-4] In addition, water is an excellent solvent which gives rise to rich acid base chemistry[5-9] and therefore plays a central role in the mechanisms by which ions and protons are transported in biochemistry[10-12] and electrochemistry[13-15]. While computer simulations have taken a key role in unraveling some of water's intriguing properties,[16-24] the methodologies available are limited either by their computational cost, lack of sufficient accuracy and/or applicability for reactive systems. Therefore, the development of new theoretical models which are more accurate, transferable and efficient is highly desirable.

Water models have evolved tremendously over the last decades starting with the early simple rigid point charge models such as SPC[25] and TIP3P[26] model, to later TIP4P-EW[27] and TIP5P[28] models which include Ewald summation and off-atom charge sites. More advanced models include electrostatic polarization which has been shown to increase the transferability among the different phases of water.[29] Currently state-of-the-art water models such as MB-UCB[30] and MB-Pol[31] are parameterized solely on high quality *ab initio* cluster data and are designed to account for the many-body physics of the electronic degrees of freedom, with such good accuracy as to require treatment of nuclear quantum effects.[32-33] While showing high accuracy, these models are only applicable for non-reactive scenarios and cannot account for proton transport and dissolution which is the basis for water's unique acid-base chemistry.

In order to study such systems, reactive dissociable models are required. Several dedicated force fields have been developed to study proton transfer in water such as models based on the central force field[34], molecular mechanics with proton transfer force field and reactive molecular dynamics[35], and valence bond models such as MS-EVB[36]. However, these models are designed to solely treat proton transport and extension of these models to more complicated reactive chemistry and electrochemistry is not straightforward. Bond order reactive force fields (BO-RFF) provide a more general approach to account for chemical reactivity within classical models. Early generation BO-RFF's such as the Tersoff[37] and REBO[38] potentials introduced the concept of bond order to describe the different phases of carbon systems. The AIREBO potential extends these early potentials by the addition of intermolecular interactions and a flexible torsional term for switching between the different hybridization states of carbon.[39] This allowed for a transferable BO-RFF that can describe

the different solid, liquid and gas phases of hydrocarbons within one theoretical framework. This soon led to BO-RFF models such as the ReaxFF[40] and COMB[41] methods which moved beyond just hydrocarbons, and combined with charge equilibration methods (QEq)[42-43], now accounted for the charge rearrangement as bonds break and form.

However, QEq methods do give rise to some notable shortcomings including lack of out-of-plane polarization, unphysical long-range charge transfer, and incorrect dissociation into ionic fragments that limit their accuracy in applications such as proton transfer, acid/base chemistry and electrocatalysis. Recognizing these limitations, several new approaches to develop classical models which can account for redox reactions rely on either explicit treatment of electrons[44-45] or empirical electron transfer probabilities[46]. Our recently developed coarse-grained electron model (C-GeM)[47] is an alternative approach for evaluating the electrostatic potential of molecules utilizing explicit coarse-grained electrons. It has been shown to predict with high accuracy the electrostatic potential surface of various molecules containing the elements C, H, O, and Cl (and is currently being developed for other first row elements), and allows a straightforward description of dissociation of molecules to integer charged fragments, out of plane polarization, and more physical descriptions of short-ranged charge transfer.

In this work we develop a new approach for reactive force fields by replacing the QEq method[42] term with C-GeM to derive a more accurate ReaxFF model for water, and compare its performance with two recent ReaxFF water models, the second generation ReaxFF water model[48] and ReaxFF for weak water hydrocarbon interactions[49] which use the QEq method. We characterize the ReaxFF/C-GeM water model in regard to its dissociative and energetic properties on small cluster data, as well as its condensed phase properties not just at ambient conditions, but its temperature dependence for both density and transport properties as well. This work lays the foundation for a reactive force field which not only remedies the shortcomings of QEq, but through the explicit treatment of electrons, should be more *transferable* for modelling a range of reactive chemistries such as redox reactions and aqueous phase chemistry in future applications.

THEORY

The original ReaxFF force field is comprised of terms which can be classified into bonded and non-bonded terms, for which the bonded terms account for breaking and forming of bonds given their hybridization state.[40] The non-bonded terms consist of a van der Waals term which accounts for dispersion and Pauli repulsion interactions as well as an electrostatic term treated with the QEq

model.[40] Here we describe in more detail the modifications we made to ReaxFF, that at its most basic description is the replacement of the QEq model for C-GeM. The supplementary material contains information on the numerical protocols used to simulate ReaxFF/C-GeM and its water properties.

Pauli Repulsion and Dispersion: For the ReaxFF/C-GeM potential we slightly modified the original van der Waals term to obtain a more coherent separation between Pauli repulsion and dispersion interactions. In our model, the attractive part of the Morse potential has been discarded, and only the shielded exponential term is used to treat Pauli repulsion

$$E_{Pauli} = \sum_{i=1}^{n}\sum_{j<i}^{n} Tap(r_{ij}) \cdot \left(D_{ij} \cdot exp\left(\alpha_{ij} \left(1 - \frac{f_{13}(r_{ij})}{r_{vdW}} \right) \right) \right) \tag{1}$$

$$f_{13}(r_{ij}) = \left(r_{ij}^{P_{vdW1}} + \left(\frac{1}{\gamma_W} \right)^{P_{vdW1}} \right)^{\frac{1}{P_{vdW1}}}$$

where the sum is over n atoms in the system, r_{ij} is the distance between atom i and j, D_{ij} is a pre-exponential parameter determining the magnitude of the repulsive interactions, r_{vdW} determines the onset of the repulsive interaction and $f_{13}(r_{ij})$ is a shielding function acting at short range. The entirety of the repulsive interaction is tapered to go to zero as manifested in $Tap(r_{ij})$. To account for dispersion, we used the low-gradient correction which was originally used as a dispersion correction term for energetic materials[50], with the following functional form

$$E_{disp} = \sum_{i=1}^{n}\sum_{j<i}^{n} Tap(r_{ij}) \cdot \left(-\frac{C_{lg}}{r_{ij}^6 + R_{eij}^6} \right) \tag{2}$$

where C_{lg} is the dispersion coefficient between atoms i and j and R_{eij} is a parameter dictating the van der Waals shielding at short distance.

C-GeM: In C-GeM atoms are divided into positive charged cores and negative shells. The concept behind C-GeM is that the shell positions are minimized in the field of the cores, such that the final core-shell configuration generates the electrostatic potential of the molecule. In C-GeM the cores and shells are treated as gaussian charges and given a charge of +1 and -1 for the cores and shells respectively, the electrostatic interaction between two Gaussian charges i and j given by:

$$E_{ij}^{elec}(r_{ij}) = \frac{q_i \cdot q_j}{r_{ij}} erf\left(\sqrt{\frac{\alpha_i \cdot \alpha_j}{\alpha_i + \alpha_j}} r_{ij} \right) \quad where \quad \alpha_i = \frac{\lambda}{2 * R_i^2} \tag{3}$$

Here q_i and q_j are the charges and α_i and α_j determine the width of the gaussian distribution of particles i and j respectively. The width of the gaussian distribution α_i is determined by the global parameter λ and the particle radius R_i.

In addition to electrostatic interactions, C-GeM uses a Gaussian term between core-shell and shell-shell interactions to control the magnitude of the interaction, defined as the electronegativity of a given atom type while the shell-shell interaction is a fitted parameter.

$$E_{ij}^{Gauss}(r_{ij}) = A_i e^{-\gamma_i \cdot r_{ij}^2} \qquad where \qquad \gamma_i = \frac{\omega_m}{2 \cdot R_i} \tag{4}$$

where ω_m is a global parameter, m corresponds to either cores or shells and A_i is obtained from the difference between the electrostatic energy and the electronegativity of a given atom type, χ_i so the that the total core-shell interaction energy (electrostatic + Gaussian) will equal the atom's electronegativity as given by:

$$A_i = \chi_i - \frac{2q_i \cdot q_j}{\pi}\left(\sqrt{\frac{\alpha_i \cdot \alpha_j}{\alpha_i + \alpha_j}}\right) \tag{5}$$

For core-core interaction $A_i = 0$ as the Gaussian term is only applied for core-shell and shell-shell interactions. The total C-GeM interaction energy is given by:

$$E_{CGeM} = \sum_{i=1}^{N}\sum_{j<i}^{N} Tap(r_{ij}) \cdot \left(E_{ij}^{elec}(r_{ij}) + E_{ij}^{Gauss}(r_{ij})\right) \tag{6}$$

Where N is the number of cores + shells in the system and a similar tapering function is used to modulate the lengthscale over which the interaction is operative. In this work we have used a tapering function of the form used in ReaxFF

$$Tap(r_{ij}) = \frac{20}{R_{cut}^7} r_{ij}^7 - \frac{70}{R_{cut}^6} r_{ij}^6 + \frac{84}{R_{cut}^5} r_{ij}^5 - \frac{35}{R_{cut}^4} r_{ij}^4 + 1 \tag{7}$$

And using $R_{cut} = 10$Å for all reported results.

Force field training: The ReaxFF/C-GeM potential energy surface was trained against high quality density functional theory (DFT) data at the ωB97x-v functional using aug-cc-pvqz[51] level of theory. Single point energy calculations were performed and compared to DFT by minimizing the shell positions self consistently at each configuration using the FIRE 2.0[52] algorithm. Our training data set is comprised of water monomer dissociation and bending curves, intermolecular interactions of the water dimer and pentamer, and proton hopping dissociation curves for the hydronium and hydroxide ions. The parameters were fitted by minimizing the root mean square deviation of the DFT

and ReaxFF/C-GeM energies. We note that although our focus was on fitting to DFT data, manual adjustment of parameters and multiple rounds of parameter fitting were necessary for obtaining a sufficient agreement with experimental bulk water properties. In addition, we compare the potential energy surface (PES) of the current model denoted as "ReaxFF/C-GeM" with two recent ReaxFF water models: the ReaxFF-2nd water force field optimized for hydroxide diffusion[48] and the ReaxFF-weak optimized for functionalized hydrocarbon/water interactions[49].

RESULTS

Figure 1a shows the hydrogen dissociation curve of a single water molecule, in which all three reactive force fields are slightly underbound, although the ReaxFF/C-GeM model shows better agreement with the DFT benchmark throughout the entire curve. In addition, the C-GeM energy comprises approximately 32.5% of the total ReaxFF/C-GeM binding energy and contributes to stabilization of the minimum at 0.96 Å, in good agreement with the DFT equilibrium distance.

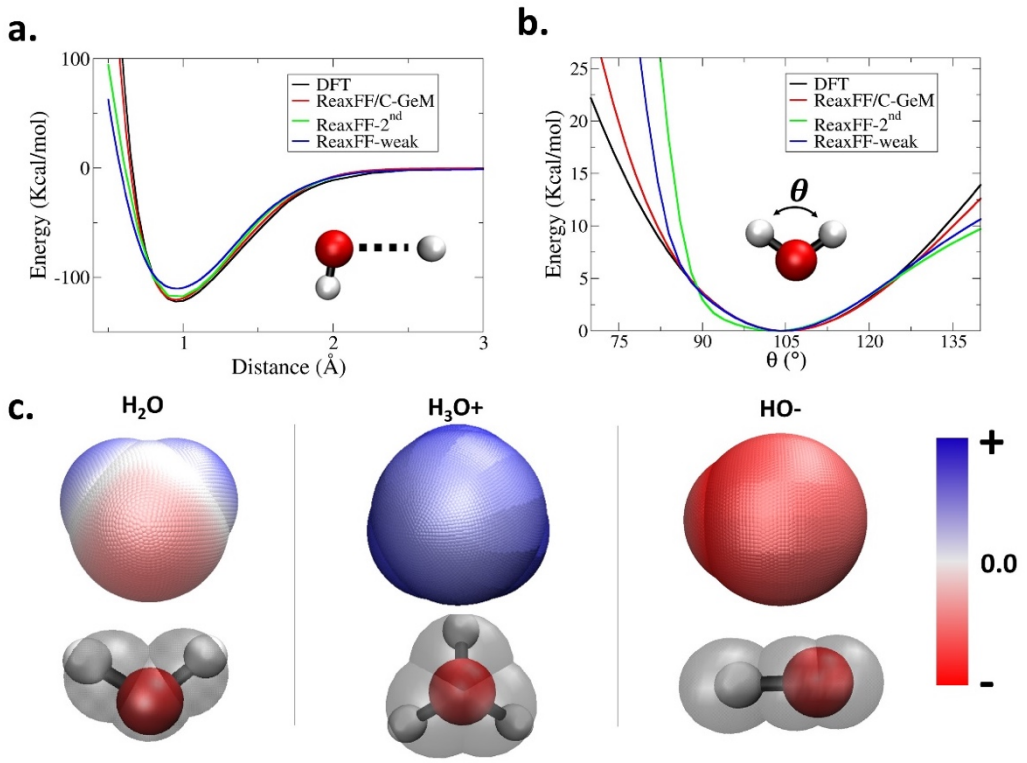

Figure 1: *Properties of a single water molecule for ReaxFF/C-GeM compared to ReaxFF-2nd and DFT.* (a) Bond dissociation curve of a hydrogen atom from a water molecule and (b) energy as a function of valance angle comparing DFT (black), ReaxFF/C-GeM (red), ReaxFF-^{2nd} (green) and ReaxFF-weak (blue). (c) top: Electrostatic potential surface bottom: Schematic presentation of the C-GeM core-shell model of a water molecule, hydronium anion and hydroxide cation. The scale coloring of the electrostatic potential is in arbitrary units.

Figure 1b plots the bending energy, again showing good agreement between ReaxFF/C-GeM and DFT, whereas both the ReaxFF-2nd and ReaxFF-weak models have a slightly smaller equilibrium value of 103.2° and 104.2° respectively. Figure 1c presents a schematic presentation of the optimized core and shell positions and corresponding electrostatic potential surfaces for water and the hydronium and hydroxide ions as predicted by the ReaxFF/C-GeM model. It can be seen that the shells move toward the oxygens due to their larger electronegativity forming a negative charge around the oxygens and positive charge around the hydrogens. In addition, it can be seen that the shells organize between the O-H bonds of the hydronium cation forming a symmetric molecule.

Accurate modeling of the hydrogen bond in water is essential for capturing water's unique bulk properties. While the previous ReaxFF-2nd and ReaxFF-weak water models require a separate hydrogen bond term, the displacement of electronic shells around the atomic cores in C-GeM recovers excellent directional hydrogen-bonding, and thus we eliminated the original hydrogen bond term in ReaxFF/C-GeM. Figure 2a plots the resulting intermolecular binding energy of the water dimer, in which the ReaxFF/C-GeM model underestimates the binding energy by 0.65 kcal/mole whereas both the ReaxFF-2nd and ReaxFF-weak models overestimates the binding energy by 1.3 kcal/mole and 1.1 kcal/mol respectively relative to the DFT result. Figure 2b plots the barrier for rotation around the water dimer hydrogen bond, showing that ReaxFF/C-GeM underestimates the barrier by 0.35 kcal/mole whereas the ReaxFF-2nd and ReaxFF-weak overestimate the barrier by 0.79 kcal/mole and 0.78 kcal/mol respectively relative to DFT. As a validation test, Figure 2c plots the correlation between DFT and the different ReaxFF water models energies of 50 dimer and 50 pentamer structures taken from molecular dynamics trajectories of the MB-UCB model[30]. It is seen that the ReaxFF/C-GeM model slightly underestimates the energies with respect to DFT, with RMSE of 1.9 kcal/mol, whereas ReaxFF-2nd and ReaxFF-weak energies overestimate the DFT energy with RMSE of 6.4 kcal/mol and 2.87kcal/mol respectively. A final validation to test the accuracy of the reactive force field model are the binding energy calculations of water clusters of varying size as provided in Table S1. The ReaxFF/C-GeM yields good agreement with the DFT binding energies, with an average error of 3.1 kcal/mole and with random sign error. The ReaxFF-weak yields a larger but overall decent error of 5.98 kcal/mol, whereas the ReaxFF-2nd systematically overestimates the water clusters binding energy significantly.

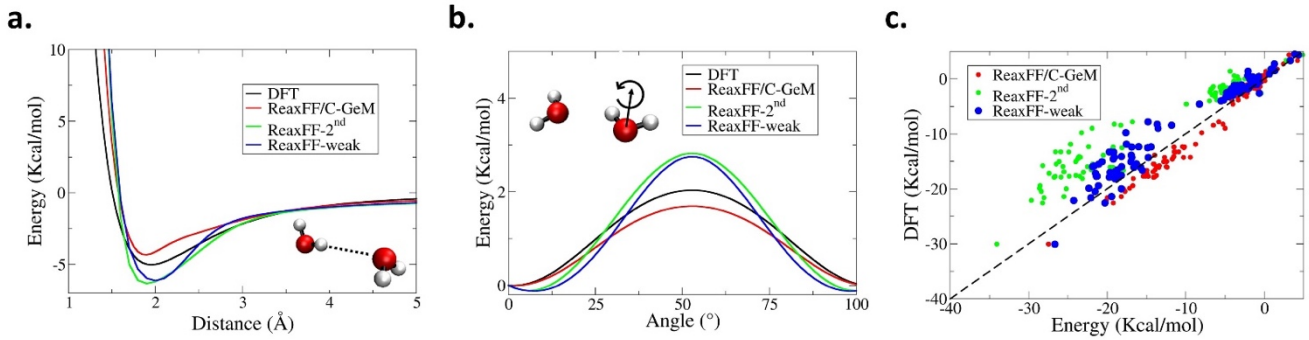

Figure 2: *Comparison of binding energies for small water clusters for ReaxFF/C-GeM, ReaxFF-2nd compared and ReaxFF-weak to DFT.* (a) Water dimer binding energy as a function of intermolecular distance. (b) Water dimer binding energy as a function of rotational angle around the hydrogen-bond. (c) Correlation between DFT and the ReaxFF water models binding energies for various dimer and pentamer water structures taken from MD simulations. DFT (black), ReaxFF/C-GeM (red), ReaxFF-2nd (green) and ReaxFF-weak (blue).

Next we consider the hydronium and hydroxide dissociative products for water. Figure 3a shows that the while the hydronium binding energy of ReaxFF/C-GeM is in reasonable agreement with the DFT result, the equilibrium distance is larger by ~0.2 Å, whereas we find that the equilibrium distance for hydroxide binding is in good agreement but with a binding energy that is higher by ~15 kcal/mole relative to DFT (Figure 3b). One limitation of the ReaxFF-2nd and ReaxFF-weak models using QEq is that we can't evaluate a system with a net charge to perform a similar analysis. Instead the hydronium and hydroxide binding energy calculations were performed by neutralizing the system with an additional ion at a very far distance from the interacting molecules. Because the optimized QEq predicts a small charge for the hydroxide and hydronium ions (–0.37e and +0.37e), the ReaxFF-2nd and ReaxFF-weak models are found to dramatically underestimate the intermolecular binding energy for H_3O^+ and OH^- as seen in Figure 3a. In Figure S1, we plot the ReaxFF/C-GeM binding curve for two values of the taper cut-off distance showing that a cutoff of 10Å results in overestimation of the binding energy at long distances. This suggests that a more accurate scheme for long range electrostatics such as Ewald summation is necessary and will be a subject of future work for the ReaxFF/C-GeM model. The H_3O^+ and OH^- water proton hopping energy is presented in Figure 3c and Figure 3d respectively, in which the energies are evaluated relative to the minimum energy at the equilibrium O-O distance curves for DFT and ReaxFF/C-GeM. It is seen that for both H_3O^+ and OH^- there is a negligible barrier for proton transfer at the equilibrium binding distance from DFT, which is well reproduced by the ReaxFF/C-GeM model. As the distance between the molecules

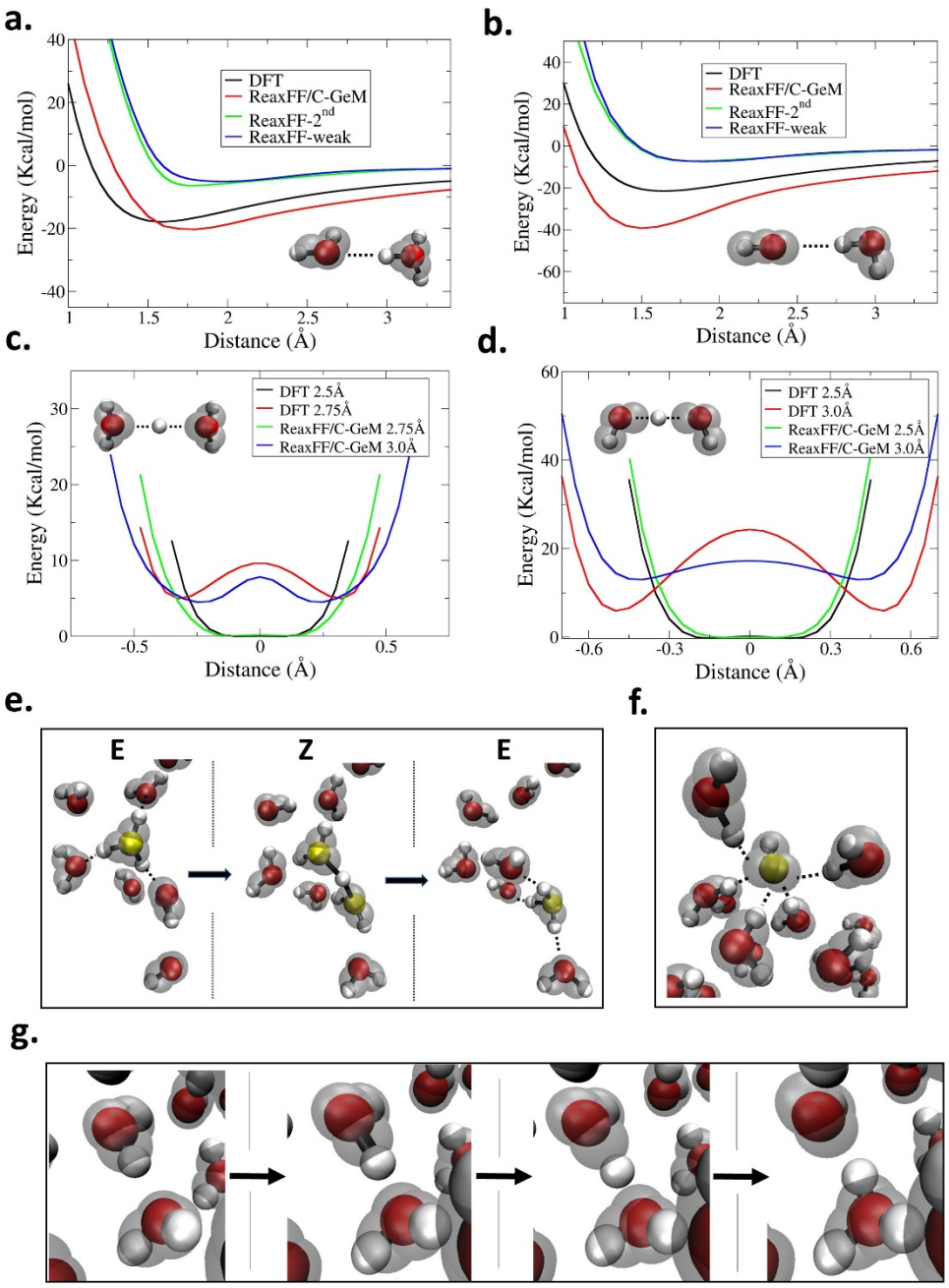

Figure 3: *Water dissociative ion interactions for ReaxFF/C-GeM, ReaxFF-2nd and ReaxFF-weak compared to DFT.* Binding energy as a function of distance between water and (a) hydronium ion, and (b) hydroxide ion. Proton transfer energy as a function of oxygen-oxygen distances between water and (c) hydronium ion and (d) hydroxide ion; the hopping energies are compared at relative oxygen-oxygen distance with respect to the equilibrium value of 2.75Å (ReaxFF/C-GeM) and 2.5Å (DFT) to be consistent with their equilibrium distances. (e) Schematic representation of a proton transfer event showing the Eigen-Zundel-Eigen mechanism and (f) Schematic presentation of hypersolvation of hydroxide with 5 water molecules, both taken from MD simulations with ReaxFF/C-GeM. (g) Schematic presentation of water dissociation to Hydronium and hydroxide ions using constrained dynamics.

increases, the ReaxFF/C-GeM model is found to underestimate the proton hopping barrier for H_3O^+ by 1.3 kcal/mol and for OH^- by 17.8 kcal/mol compared to DFT. Even so, the ReaxFF/C-GeM model is shown to exhibit the hydronium Eigen-Zundle-Eigen proton transfer mechanism (Figure 3e) consistent with experiment, and reproduces the hyper-solvated structure of the hydroxide ion (Figure 3f) which has been attributed to its lower diffusion constant. When compared to the experimental diffusion constants for the water hydronium (0.93 $Å^2$/ps) and hydroxide (0.56 $Å^2$/ps) ions, we find that ReaxFF/C-GeM underestimates the transport values, yielding 0.83 $Å^2$/ps for hydronium and 0.40 $Å^2$/ps for hydroxide, although their ratio is in good agreement with experiment. The ReaxFF-2nd model only slightly overestimates the hydronium diffusion constant (1.04 $Å^2$/ps) but predicts hydroxide diffusion that is ~40% faster (0.78 $Å^2$/ps), which is likely due to its reported underbinding of the water-hydroxide complex. In order to demonstrate the ReaxFF/C-GeM capability to predict the correct charges for water dissociation to ionic products in solution and neutral in the gas phase, we have conducted constraint dynamics simulations of water dissociation in both solution and gas. Figure 3g presents snapshots taken from an MD trajectory of a 20-water cluster where one hydrogen core was constrained to dissociate from a water molecule. It is shown that upon dissociation the hydrogen's shell prefers to stay on the OH fragment yielding the OH- anion and the dissociating hydrogen core binds to a nearby water molecule yielding the H_3O+ cation. In contrast, for a single water molecule in vacuum, dissociation leads to two neutral products of OH and H.

Finally, we demonstrate the capability of the ReaxFF/C-GeM model to reproduce various structural, thermodynamic, and dynamic properties of bulk water. Figure 4a compares the oxygen-oxygen radial distribution function at 300K/1atm, in which the ReaxFF/C-GeM water structure is overall in good agreement with the experiment, although it presents a slightly overstructured hydrogen bonded network for bulk water as evidenced by higher peaks at the first and second hydration shells. The ReaxFF-weak presents the overall best water structure out of the three models characterized by a slightly underestimated first peak whereas the ReaxFF-2nd is more structured with the first peak shifted to small distance compared to ReaxFF/C-GeM and experiment. Overall the ReaxFF/C-GeM model reproduces the IR spectra of liquid water reasonably well with respect to both the intensity and peak location (Figure 4d), in which the high frequency OH vibrational stretch and low frequency vibrational modes are both redshifted by ~130 cm^{-1} whereas the bending mode is blueshifted by ~64 cm^{-1}. Both the ReaxFF-2nd and ReaxFF-weak models exhibit decent vibrational frequencies however they dramatically underestimates the intensity of the OH stretch even with the

addition of quantum corrections which typically increase the intensity of the high frequency vibrational modes.

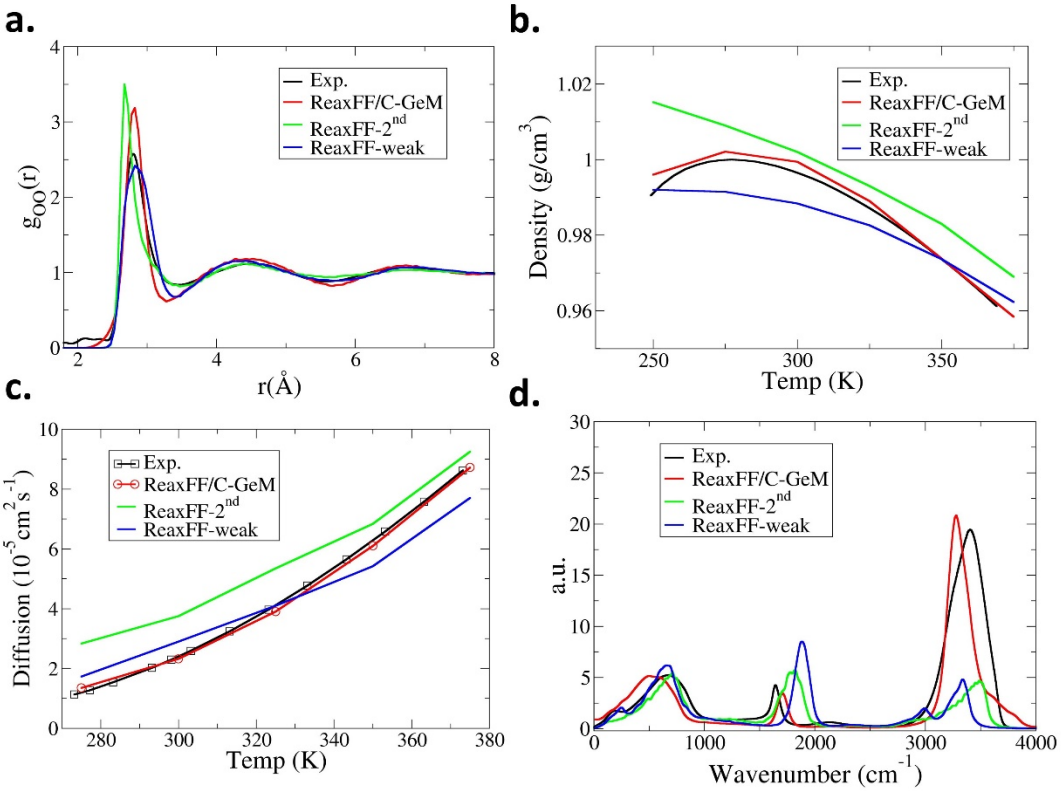

Figure 4. Comparison of various water properties with experiment: a. Oxygen-Oxygen radial distribution. b. Density as a function of temperature. c. Diffusion as a function of temperature. d. IR spectra. Comparing experiment (black), ReaxFF/C-GeM (red), ReaxFF-2*nd* (green) and ReaxFF-weak (blue).

An important aspect in the evaluation of any water model is its characterization over more than just one state point, and we have evaluated both reactive models over a range of temperatures in the NPT ensemble as shown in Figures 4b and 4c. We find that the ReaxFF/C-GeM model predicts a temperature of maximum density (TMD) at 279 K and a density of 0.999 g/cm^3 at 300K, in excellent agreement with the experimental values of 277 K and 0.997 g/cm^3, respectively, and it shows an excellent temperature dependence of the water molecule diffusion coefficient as well. In contrast, both the ReaxFF-2nd and ReaxFF-weak, which were parameterized to reproduce only ambient bulk water properties, show no apparent TMD at temperatures above 250K. While the ReaxFF-2nd overestimates the diffusion coefficient with respect to experiment at all temperatures the ReaxFF-weak presents an overall improvement over the ReaxFF-2nd.

DISCUSSION AND CONCLUSION

One of the primary goals of this work is to develop the non-bonded interactions of a reactive force field toward the better accuracy exhibited by more advanced non-reactive water models such as MB-UCB[30] and MB-Pol[53-54]. In this work we present a new reactive force field for liquid water that embeds the bond order framework of the ReaxFF force field[40] within our recently developed C-GeM model[47] that accounts for permanent electrostatics, polarization, and charge transfer for reactive systems. The use of C-GeM remedies many of the shortcomings associated with QEq used with ReaxFF such as unphysical long-range charge transfer, lack of out-of-plane polarization, and the inability to correctly dissociate to integer charge fragments. Furthermore, the C-GeM model allows for a straightforward description of charged systems and distinction between chemical species such as the hydroxy radical and hydroxide ion that will be important for any application involving a reactive aqueous system, and thus should benefit its general transferability.

When characterized at ambient states, the ReaxFF/C-GeM model is found to produce good structural quantities and quality vibrational spectra of bulk water. But a second goal of this work is to also raise the bar of characterization of a reactive force field, in particular evaluating its performance in the experimentally relevant NPT ensemble over a large range of temperatures for water. The ReaxFF/C-GeM water model was shown to describe the temperature dependence of bulk water diffusion constants and water density with a level of accuracy approaching that of many-body non-reactive force fields. The ReaxFF/C-GeM model developed here is a first step towards an accurate reactive force field for modeling redox and acid-base chemistry, and the explicit treatment of electrons will permit study of both electron or proton transfer processes between molecules relevant to electrochemistry and related applications.

ACKNOWLEDGEMENT

The authors thank the National Science Foundation for support under Grant No. CHE- 1955643. This research used the computational resources of the National Energy Research Scientific Computing Center, a DOE Office of Science User Facility supported by the Office of Science of the U.S. Department of Energy under Contract No. DE-AC02-05CH11231.

SUPPORTING INFORMATION

The SI contains computational information including, simulation details, extended Lagrangian formalism and infra-red spectrum calculation. In additions the SI contains comparison of different

tapering cut-off values on water ion interaction, a table comparing energies of small water clusters and the parameters used in the current paper.

REFERENCES

1. Debenedetti, P. G. One substance, two liquids? *Nature* **1998,** *392* (6672), 127-128.
2. Ball, P. Water: Water - an enduring mystery. *Nature* **2008,** *452* (7185), 291-292.
3. Hauner, I. M.; Deblais, A.; Beattie, J. K.; Kellay, H.; Bonn, D. The dynamic surface tension of water. *J. Phys. Chem. Lett.* **2017,** *8* (7), 1599-1603.
4. Millot, M.; Coppari, F.; Rygg, J. R.; Correa Barrios, A.; Hamel, S.; Swift, D. C.; Eggert, J. H. Nanosecond X-ray diffraction of shock-compressed superionic water ice. *Nature* **2019,** *569* (7755), 251-255.
5. Eigen, M. Proton Transfer Acid-Base Catalysis + Enzymatic Hydrolysis .I. Elementary Processes. *Angew. Chem. Int. Ed.***1964,** *3* (1), 1-&.
6. Mohammed, O. F.; Pines, D.; Dreyer, J.; Pines, E.; Nibbering, E. T. J. Sequential proton transfer through water bridges in acid-base reactions. *Science* **2005,** *310* (5745), 83-86.
7. Thamer, M.; De Marco, L.; Ramasesha, K.; Mandal, A.; Tokmakoff, A. Ultrafast 2D IR spectroscopy of the excess proton in liquid water. *Science* **2015,** *350* (6256), 78-82.
8. Agmon, N.; Bakker, H. J.; Campen, R. K.; Henchman, R. H.; Pohl, P.; Roke, S.; Thamer, M.; Hassanali, A. Protons and Hydroxide Ions in Aqueous Systems. *Chem. Rev.* **2016,** *116* (13), 7642-7672.
9. Wolke, C. T.; Fournier, J. A.; Dzugan, L. C.; Fagiani, M. R.; Odbadrakh, T. T.; Knorke, H.; Jordan, K. D.; McCoy, A. B.; Asmis, K. R.; Johnson, M. A. Spectroscopic snapshots of the proton-transfer mechanism in water. *Science* **2016,** *354* (6316), 1131-1135.
10. Cooke, R.; Kuntz, I. D. The properties of water in biological systems. *Ann. Rev. Biophys. Bioeng.* **1974,** *3* (0), 95-126.
11. Chaplin, M. Opinion - Do we underestimate the importance of water in cell biology? *Nature Rev. Mol. Cell Bio.* **2006,** *7* (11), 861-866.
12. Ball, P. Water is an active matrix of life for cell and molecular biology. *Proc. Natl. Acad. Sci. USA* **2017,** *114* (51), 13327-13335.
13. Zhao, C. M.; Zheng, W. T. A review for aqueous electrochemical supercapacitors. *Front. Energy Res.* **2015**.
14. Zhong, C.; Deng, Y. D.; Hu, W. B.; Qiao, J. L.; Zhang, L.; Zhang, J. J. A review of electrolyte materials and compositions for electrochemical supercapacitors. *Chem. Soc. Rev.* **2015,** *44* (21), 7484-7539.
15. Xia, L.; Yu, L. P.; Hu, D.; Chen, G. Z. Electrolytes for electrochemical energy storage. *Mater Chem Front* **2017,** *1* (4), 584-618.
16. Pertsemlidis, A.; Saxena, A. M.; Soper, A. K.; Head-Gordon, T.; Glaeser, R. M. Direct evidence for modified solvent structure within the hydration shell of a hydrophobic amino acid. *Proc. Natl. Acad. Sci. USA* **1996,** *93* (20), 10769-74.

17. Geissler, P. L.; Dellago, C.; Chandler, D.; Hutter, J.; Parrinello, M. Autoionization in liquid water. *Science* **2001,** *291* (5511), 2121-2124.
18. Matsumoto, M.; Saito, S.; Ohmine, I. Molecular dynamics simulation of the ice nucleation and growth process leading to water freezing. *Nature* **2002,** *416* (6879), 409-413.
19. Yoo, S.; Apra, E.; Zeng, X. C.; Xantheas, S. S. High-Level Ab Initio Electronic Structure Calculations of Water Clusters (H2O)_16 and (H2O)_17: A New Global Minimum for (H2O)_16. *J. Phys. Chem. Lett.* **2010,** *1* (20), 3122-3127.
20. Clark, G. N.; Hura, G. L.; Teixeira, J.; Soper, A. K.; Head-Gordon, T. Small-angle scattering and the structure of ambient liquid water. *Proc. Natl. Acad. Sci. USA* **2010,** *107* (32), 14003-7.
21. Hassanali, A.; Prakash, M. K.; Eshet, H.; Parrinello, M. On the recombination of hydronium and hydroxide ions in water. *Proc. Natl. Acad. Sci. USA* **2011,** *108* (51), 20410-5.
22. Haji-Akbari, A.; Debenedetti, P. G. Computational investigation of surface freezing in a molecular model of water. *Proc. Natl. Acad. Sci. USA* **2017,** *114* (13), 3316-3321.
23. Chen, M.; Zheng, L.; Santra, B.; Ko, H. Y.; DiStasio, R. A., Jr.; Klein, M. L.; Car, R.; Wu, X. Hydroxide diffuses slower than hydronium in water because its solvated structure inhibits correlated proton transfer. *Nature Chem.* **2018,** *10* (4), 413-419.
24. Demerdash, O.; Wang, L.-P.; Head-Gordon, T. Advanced models for water simulations. *WIREs Comput. Mol. Sci.* **2018,** *8* (1), e1355.
25. Berendsen, H. J. C., Postma, J. P. M., van Gunsteren, W. F., and Hermans, J. *Intermolecular Forces*. 1981.
26. Jorgensen, W. L. Quantum and Statistical Mechanical Studies of Liquids .10. Transferable Intermolecular Potential Functions for Water, Alcohols, and Ethers - Application to Liquid Water. *J. Am. Chem. Soc.* **1981,** *103* (2), 335-340.
27. Horn, H. W.; Swope, W. C.; Pitera, J. W.; Madura, J. D.; Dick, T. J.; Hura, G. L.; Head-Gordon, T. Development of an improved four-site water model for biomolecular simulations: TIP4P-Ew. *J. Chem. Phys.* **2004,** *120* (20), 9665-9678.
28. Mahoney, M. W.; Jorgensen, W. L. A five-site model for liquid water and the reproduction of the density anomaly by rigid, nonpolarizable potential functions. *J. Chem. Phys.* **2000,** *112* (20), 8910-8922.
29. Demerdash, O.; Wang, L. P.; Head-Gordon, T. Advanced models for water simulations. *WIREs Comput. Mol. Sci.* **2018,** *8* (1).
30. Das, A. K.; Urban, L.; Leven, I.; Loipersberger, M.; Aldossary, A.; Head-Gordon, M.; Head-Gordon, T. Development of an Advanced Force Field for Water Using Variational Energy Decomposition Analysis. *J. Chem. Theory Comput.* **2019,** *15* (9), 5001-5013.
31. Babin, V.; Leforestier, C.; Paesani, F. Development of a "First-Principles" Water Potential with Flexible Monomers: Dimer Potential Energy Surface, VRT Spectrum, and Second Virial Coefficient (vol 9, pg 5395, 2013). *J. Chem. Theory Comput.* **2014,** *10* (8), 3585-3585.
32. Pereyaslavets, L.; Kurnikov, I.; Kamath, G.; Butin, O.; Illarionov, A.; Leontyev, I.; Olevanov, M.; Levitt, M.; Kornberg, R. D.; Fain, B. On the importance of accounting for nuclear quantum effects in ab initio calibrated force fields in biological simulations (vol 115, pg 8878, 2018). *Proc. Natl. Acad. Sci. USA* **2018,** *115* (39), E9258-E9258.
33. Markland, T. E.; Ceriotti, M. Nuclear quantum effects enter the mainstream. *Nature Rev. Chem.* **2018,** *2* (3).
34. Asthana, A.; Wheeler, D. R. A polarizable reactive force field for water to enable molecular dynamics simulations of proton transport. *J. Chem. Phys.* **2013,** *138* (17).

35. Xu, Z.-H.; Meuwly, M. Multistate Reactive Molecular Dynamics Simulations of Proton Diffusion in Water Clusters and in the Bulk. *J. Phys. Chem. B* **2019,** *123* (46), 9846-9861.
36. Wu, Y. J.; Chen, H. N.; Wang, F.; Paesani, F.; Voth, G. A. An improved multistate empirical valence bond model for aqueous proton solvation and transport. *J. Phys. Chem. B* **2008,** *112* (2), 467-482.
37. Tersoff, J. New Empirical-Approach for the Structure and Energy of Covalent Systems. *Phys. Rev. B* **1988,** *37* (12), 6991-7000.
38. Brenner, D. W. Empirical Potential for Hydrocarbons for Use in Simulating the Chemical Vapor-Deposition of Diamond Films. *Phys. Rev. B* **1990,** *42* (15), 9458-9471.
39. Brenner, D. W.; Shenderova, O. A.; Harrison, J. A.; Stuart, S. J.; Ni, B.; Sinnott, S. B. A second-generation reactive empirical bond order (REBO) potential energy expression for hydrocarbons. *J Phys-Condens Mat* **2002,** *14* (4), 783-802.
40. van Duin, A. C. T.; Dasgupta, S.; Lorant, F.; Goddard, W. A. ReaxFF: A reactive force field for hydrocarbons. *J Phys Chem A* **2001,** *105* (41), 9396-9409.
41. Yu, J.; Sinnott, S. B.; Phillpot, S. R. Charge optimized many-body potential for theSi/SiO2system. *Phys Rev B* **2007,** *75* (8).
42. Mortier, W. J.; Ghosh, S. K.; Shankar, S. Electronegativity Equalization Method for the Calculation of Atomic Charges in Molecules. *J Am Chem Soc* **1986,** *108* (15), 4315-4320.
43. Rappe, A. K.; Goddard, W. A. Charge Equilibration for Molecular-Dynamics Simulations. *J Phys Chem-Us* **1991,** *95* (8), 3358-3363.
44. Islam, M. M.; Kolesov, G.; Verstraelen, T.; Kaxiras, E.; van Duin, A. C. eReaxFF: A Pseudoclassical Treatment of Explicit Electrons within Reactive Force Field Simulations. *J Chem Theory Comput* **2016,** *12* (8), 3463-72.
45. Bai, C.; Kale, S.; Herzfeld, J. Chemistry with semi-classical electrons: reaction trajectories auto-generated by sub-atomistic force fields. *Chem Sci* **2017,** *8* (6), 4203-4210.
46. Dapp, W. B.; Muser, M. H. Redox reactions with empirical potentials: atomistic battery discharge simulations. *J Chem Phys* **2013,** *139* (6), 064106.
47. Leven, I.; Head-Gordon, T. C-GeM: Coarse-Grained Electron Model for Predicting the Electrostatic Potential in Molecules. *J Phys Chem Lett* **2019,** *10* (21), 6820-6826.
48. Zhang, W.; van Duin, A. C. T. Second-Generation ReaxFF Water Force Field: Improvements in the Description of Water Density and OH-Anion Diffusion. *The Journal of Physical Chemistry B* **2017,** *121* (24), 6021-6032.
49. Zhang, W.; van Duin, A. C. T. Improvement of the ReaxFF Description for Functionalized Hydrocarbon/Water Weak Interactions in the Condensed Phase. *The Journal of Physical Chemistry B* **2018,** *122* (14), 4083-4092.
50. Liu, L.; Liu, Y.; Zybin, S. V.; Sun, H.; Goddard, W. A. ReaxFF-lg: Correction of the ReaxFF Reactive Force Field for London Dispersion, with Applications to the Equations of State for Energetic Materials. *The Journal of Physical Chemistry A* **2011,** *115* (40), 11016-11022.
51. Mardirossian, N.; Head-Gordon, M. omega B97X-V: A 10-parameter, range-separated hybrid, generalized gradient approximation density functional with nonlocal correlation, designed by a survival-of-the-fittest strategy. *Phys Chem Chem Phys* **2014,** *16* (21), 9904-9924.
52. Guenole, J.; Nohring, W. G.; Vaid, A.; Houlle, F.; Xie, Z. C.; Prakash, A.; Bitzek, E. Assessment and optimization of the fast inertial relaxation engine (FIRE) for energy minimization in atomistic simulations and its implementation in LAMMPS. *Comp Mater Sci* **2020,** *175*.
53. Babin, V.; Medders, G. R.; Paesani, F. Toward a Universal Water Model: First Principles Simulations from the Dimer to the Liquid Phase. *J Phys Chem Lett* **2012,** *3* (24), 3765-3769.

54. Reddy, S. K.; Straight, S. C.; Bajaj, P.; Huy Pham, C.; Riera, M.; Moberg, D. R.; Morales, M. A.; Knight, C.; Gotz, A. W.; Paesani, F. On the accuracy of the MB-pol many-body potential for water: Interaction energies, vibrational frequencies, and classical thermodynamic and dynamical properties from clusters to liquid water and ice. *J Chem Phys* **2016,** *145* (19), 194504.